Applied Catalysis B: Environmental 92 (2009) 422–428

Contents lists available at ScienceDirect

Applied Catalysis B: Environmental

journal homepage: www.elsevier.com/locate/apcatb

Effect of hydrocarbon species on no oxidation over diesel oxidation catalysts

Karishma Irani [a], William S. Epling [a,*], Richard Blint [b]

[a] Department of Chemical Engineering, University of Waterloo, Waterloo, ON, Canada
[b] General Motors R&D Center, Chemical and Environmental Sciences Laboratory, Michigan, USA

ARTICLE INFO

Article history:
Received 19 June 2009
Received in revised form 24 August 2009
Accepted 26 August 2009
Available online 1 September 2009

Keywords:
Diesel oxidation catalyst
Hydrocarbon poisoning
NO oxidation

ABSTRACT

The effect of propylene concentration on NO oxidation as a function of temperature and position over a model Pt-Pd/Al_2O_3 diesel oxidation catalyst was investigated. Propylene had an apparent inhibition effect on NO oxidation. This apparent inhibition is a result of NO_2, as the NO oxidation product, acting as an oxidant in the reaction with propylene. This was verified with experiments that included NO_2, and a resulting significant temperature decrease in the onset of NO_2 reduction when propylene was present. Furthermore, increasing amounts of propylene further decreased the NO_2 reduction temperature. Similar results were observed with m-xylene and dodecane addition as well. The results also demonstrate that NO_2 was consumed preferentially relative to O_2 during hydrocarbon oxidation. With low inlet levels of O_2, the addition of NO_2 apparently inhibited propylene oxidation after the onset of NO_2 reduction. This subsequent inhibition was due to the NO formed, demonstrating that propylene results in reduced NO_2 outlet levels while NO inhibits propylene oxidation.

1. Introduction

With the recently fluctuating fuel prices and focus on fuel efficiency and emissions, there has been an increasing interest in lean-burn engines for passenger vehicles. Lean-burn engines are more fuel efficient than today's standard stoichiometric-burn gasoline vehicles. This increased fuel efficiency also results in lower CO_2 emissions. The challenge is reducing the other emissions, specifically NO_X, hydrocarbons and CO, and particulate matter in the case of diesel engines. Therefore, there has been increasing research in the area of lean-burn exhaust emissions catalysts.

A common catalyst in many proposed lean-burn and diesel exhaust gas aftertreatment systems is a diesel oxidation catalyst (DOC). Most DOCs are composed of ceramic cordierite or metal monolith supports coated with a high surface area, alumina- or zeolite-based washcoat containing highly dispersed noble metals such as Pt, Pd or a Pt/Pd blend. Compared to Pd, Pt-based DOCs are regarded as more active for oxidation reactions [1]. However, sintering of monometallic Pt DOCs is quicker in an oxygen-rich atmosphere compared to Pt/Pd formulations [2,3], and therefore Pt/Pd catalysts are also studied. It has been speculated that the reason for this improvement is that at temperatures between 300 and 700 °C the alloy undergoes oxidation to produce less mobile particles on the catalyst surface. This prevents particle growth and maintains the original highly dispersed active site surface area [2].

DOCs perform a range of functions in an integrated emission control system, including oxidation of exhaust hydrocarbons and CO. They also oxidize NO to NO_2, which is important for efficient performance of various downstream catalysts, such as NO_X storage/reduction (NSR) catalysts, selective catalytic reduction (SCR) catalysts and diesel particulate filters (DPFs). An NSR catalyst selectively stores NO_X during lean-phase operation and reduces this stored NO_X through a short, reductant-enriched (rich) phase. Several studies have proposed that NO_2 is a precursor for, or intermediate in, the trapping process [4–8] and overall, the presence of NO_2 enhances the performance of the NSR catalyst through improved NO_X storage [9–15]. SCR catalysts selectively reduce equi-molar concentrations of NO and NO_2 to N_2 in the presence of NH_3 at a faster rate than if only NO was available [16]. This observed enhancement in performance with NO_2 is the reason why most NSR and SCR catalyst systems have a DOC installed upstream. DPFs require temperatures of about 500–600 °C to oxidize diesel particulate matter, or soot, with O_2. However, NO_2 oxidizes soot at temperatures close to 350 °C [17] and thus, most soot filters also have DOCs upstream to facilitate lower temperature soot oxidation.

NO oxidation to NO_2, however, is limited by kinetics at lower temperatures and by thermodynamics at higher temperatures. NO/NO_2 equilibrium limitations are typically observed above 350 °C in NO oxidation tests [18]. Mulla et al. have studied NO oxidation kinetics over Pt/Al_2O_3 and NSR catalysts [19,20]. Their studies have demonstrated that the rate is approximately first order each in NO

* Corresponding author.
E-mail address: wepling@cape.uwaterloo.ca (W.S. Epling).

0926-3373/$ – see front matter © 2009 Elsevier B.V. All rights reserved.
doi:10.1016/j.apcatb.2009.08.022

and O_2, but has an approximate negative first order dependency on NO_2. This product inhibition imposes significant constraint on conversions. NO oxidation inhibition by NO_2 has also been observed over a Pt/SiO_2 catalyst [21]. The inhibition effect has been attributed to the high sticking coefficient of NO_2 on Pt [22,23], preventing other species from gaining access to the surface. Various studies have found that the activity of the catalyst for NO oxidation depends on the size of the Pt particle, where NO oxidation is better with larger particle size. This has been observed with Pt supported on Al_2O_3 [24–28], SiO_2 [25,26,28] and TiO_2 [29], and suggests that some amount of thermal aging may actually improve NO oxidation performance.

Diesel exhaust contains many pollutants, including unburned hydrocarbons, CO, NO_X and particulates, all of which are regulated. Depending on their relative affinity towards active catalyst sites, different hydrocarbons show different reactivities [30]. There have been studies which evaluated oxidation of mixtures of volatile organic compounds over Pt-based monolithic catalysts [31,32], however, most studies have evaluated individual hydrocarbons. Of interest for actual application is the study of competitive oxidation reactions over a DOC to understand the influence of various species on the reaction rates of the others. As an example, in H_2/CO oxidation, the addition of H_2 to a gas mixture containing CO causes a reduction in the light-off temperature of CO. It has been reported that H_2 enhances desorption of CO from Pt [33].

Another area that has not gained much attention is the effect of various hydrocarbons on NO oxidation and vice versa. One study [34] has reported that increasing the amount of either CO, NO or propylene lowers the oxidation conversions of both CO and propylene. However, the CO and propylene inhibition effect decreased with temperature while that of NO increased with temperature. Katare et al. [35] found a significant delay in NO oxidation light-off and a lower amount of NO_2 produced over a DOC, in the presence of hydrocarbons and CO, which they attributed to the competition between CO, hydrocarbons and NO for NO oxidation sites. In a subsequent study [36], the effect of hydrocarbons and CO on NO oxidation over a commercial DOC was investigated and the authors showed that with aged DOCs, reductants can facilitate the complete reduction of product NO_2 back to NO. They concluded that only once all the reductants were consumed, did the NO oxidize back to NO_2. These findings indicated that for aged DOCs, as long as hydrocarbons and CO are present in the exhaust, NO_2 can be consumed by the DOC, thus hindering the performance of the downstream devices. NO_2 reduction, and therefore the observed NO oxidation conversion, is also affected by the presence of CO, individually and together with propylene [4]. Over an NSR catalyst, CO reduced NO_2 to NO at temperatures >100 °C, thus decreasing the amount of NO_X stored on the surface. However, when propylene was present along with CO at low temperature, NO_2 reduction was actually inhibited, thus improving NO_X storage.

In this study, NO and hydrocarbon oxidation experiments were run. These experiments were performed with different gas mixtures to evaluate the effects of hydrocarbons on NO oxidation and NO on hydrocarbon oxidation. To better understand the mechanism behind the observed hydrocarbon effects on NO oxidation, experiments were also run with NO_2.

2. Experimental

A monolith-supported $Pt\text{-}Pd/Al_2O_3$ sample with 8 g/ft^3 loading, of 1:2 Pt:Pd, was used in these experiments. The sample was 35 mm in length and 20.4 mm in diameter. The sample was "aged" for 16 h at 650 °C in an air/steam mixture. The reactor consisted of a horizontal quartz tube placed inside a temperature-controlled furnace. The catalyst was wrapped with high-temperature 3 M Interam matting material to cover the gap between the catalyst and the reactor wall to ensure that no gas slipped around the sample. K-type thermocouples were used to measure temperatures at the inlet face of the catalyst, the outlet face of the catalyst and ~5 cm upstream of the sample.

The feed stream during the experiments contained different concentrations of gases including NO, NO_2, C_3H_6, C_8H_{10} and $C_{12}H_{26}$. Oxygen and H_2O were included in all experiments, with N_2 as the balance gas. The gas flow rate used was 19.06 L/min (equivalent to a space velocity of 100,000 h^{-1}). In comparing experiments with and without CO_2; no influence on the oxidation reaction rates was observed and hence CO_2 was not included in the feed stream in order to simplify mass spectrometer data analysis. Gases and gas mixtures were supplied by Praxair and were metered via calibrated Bronkhorst mass flow controllers. The mixture of gases excluding carbon-containing molecules and some N_2 was sent through a high-capacity furnace, achieving the target test temperature prior to entering the tube furnace holding the sample. This minimized any artificial axial and radial temperature gradients during experiments. Dodecane or m-xylene (laboratory grade supplied by Fisher Scientific) was injected into the quartz tube reactor using a Bronkhorst High-Tech series E-7000 Controlled Evaporator Mixer (CEM) system and part of the total N_2 flow as the carrier gas; it was not input upstream of the high-capacity furnace. When propylene was used, it was also introduced with the small amount of carrier N_2 directly into the tube reactor. This avoided any reactions between the carbon-containing species and O_2 on the hot, upstream steel tubing. Dodecane injection began at a catalyst temperature of about 120 °C. The gases exiting the reactor were maintained at >120 °C to avoid condensation.

For all experiments, the exiting gas compositions were measured using a MKS MultiGas 2030 FT-IR analyzer at approximately a 2 Hz collection rate. CO, CO_2, NO, NO_2, N_2O, NH_3, C_3H_6, C_8H_{10}, $C_{12}H_{26}$ and H_2O concentrations were measured. Preliminary tests verified accuracy of the concentrations of the NO, NO_2, N_2O and C_3H_6 to $<\pm 2$ ppm. In this work, both temperature programmed oxidation (TPO) as well as spatial resolution experiments at a steady-state inlet temperature (further described below) were performed. During each TPO experiment, the catalyst temperature was ramped at a rate of approximately 7.5 °C/min. Initially, tests with no reactant gases were performed and demonstrated that there was a maximum of 4 °C difference between the front and back of the sample during the temperature ramps. In the data shown below, the *x*-axis temperature is that of the upstream thermocouple, thereby avoiding complications from exotherm-generated heat on or in the sample. Dodecane cracking upstream of the catalyst was observed just above 300 °C via the mass spectrometer during preliminary temperature ramps and hence the results for the temperature ramps that included $C_{12}H_{26}$ are shown only to these temperatures.

Spatially resolved capillary-inlet mass spectrometry (SpaciMS) [37,38] was also used to characterize the reactions. During these experiments, a fixed inlet temperature was established and then a silica capillary, I.D. = 0.3 mm and O.D. = 0.43 mm, placed within one of the radially central channels was pulled to different positions within the catalyst channel to measure the gas species concentrations as a function of catalyst length. This was then repeated at a different temperature. The capillary was connected to a Hiden Analytical HPR 20 QIC mass spectrometer. Outside of the reactor, the capillary was heated along its entire length to avoid condensation. The gases measured by the mass spectrometer were; H_2O, NO, NO_2, O_2, C_3H_6 and CO_2. In the figures below, the conversions of NO, NO_2 and C_3H_6 are plotted. The MKS 2030 FT-IR was also used to verify calibration accuracy of the data measured by the mass spectrometer.

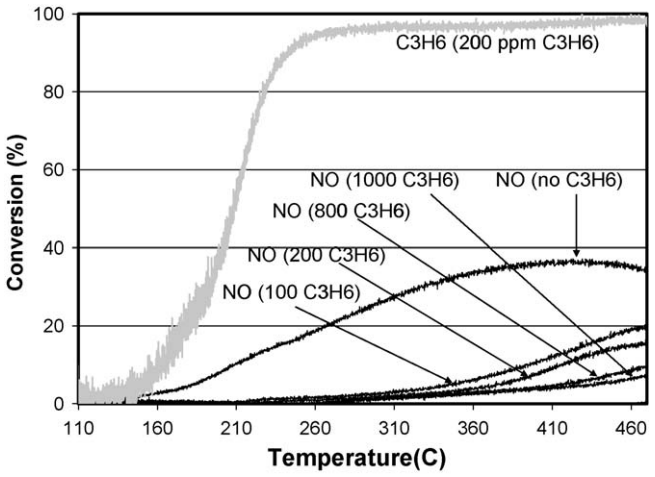

Fig. 1. NO and C_3H_6 oxidation conversion as a function of temperature and C_3H_6 concentration. The feed stream contained 200 ppm NO, 10% O_2, 5% H_2O and either 0, 100, 200, 800 or 1000 ppm C_3H_6, and a balance of N_2.

3. Results and discussion

A baseline temperature-programmed NO oxidation experiment was performed and the data are shown in Fig. 1. The NO oxidation conversion plotted is based on NO_2 made, not NO consumed. During this experiment, the temperature was ramped at ~7.5 °C/min, with 200 ppm NO, 10% O_2, 5% H_2O and a N_2 balance as the inlet gas. Oxidation conversion was measurable at 140 °C, reached a maximum of about 33% at 420 °C and then decreased. As mentioned, this trend is due to NO oxidation being kinetically limited at lower temperatures and thermodynamically limited at higher temperatures [18]. A proposed mechanism for this reaction [19,20] includes the rate of NO oxidation to be approximately negative first order in terms of NO_2 concentration. This product inhibition contributes to the low conversions observed until thermodynamic limitations are reached. The data obtained from TPO experiments containing C_3H_6 in the mixture are also presented in Fig. 1. In performing these experiments, the temperature ramp was ended at approximately 470 °C. With C_3H_6, the maximum NO oxidation conversions were measured at this maximum temperature, suggesting that higher conversions might have been attained if the temperature ramp was continued to higher temperatures. The data clearly show that the addition of C_3H_6 resulted in a significant decrease in measured NO conversion to NO_2. With the smallest C_3H_6 addition shown in this figure, 100 ppm, NO oxidation was not measured until 210 °C, and the maximum conversion was 20% at 470 °C. Increasing the C_3H_6 concentration from 100 to 1000 ppm led to further drops in NO conversion, reaching only 7% at 460 °C with 1000 ppm added. These data clearly demonstrate that C_3H_6 results in lower NO_2 produced and that as the C_3H_6 concentration was increased from 100 to 1000 ppm, NO oxidation was further hindered.

The C_3H_6 and NO oxidation conversions were also spatially resolved. Two experiments were run, one with 200 ppm NO, and one with both 200 ppm NO and 800 ppm C_3H_6. Each also contained 10% O_2, 5% H_2O and a N_2 balance, and the data are shown in Fig. 2. In the experiment with no C_3H_6, Fig. 2A, NO conversions increased down the length of the sample and with temperature. The NO conversions in the presence of C_3H_6 are plotted in Fig. 2B, with the C_3H_6 conversions also shown in Fig. 2C. As with the outlet

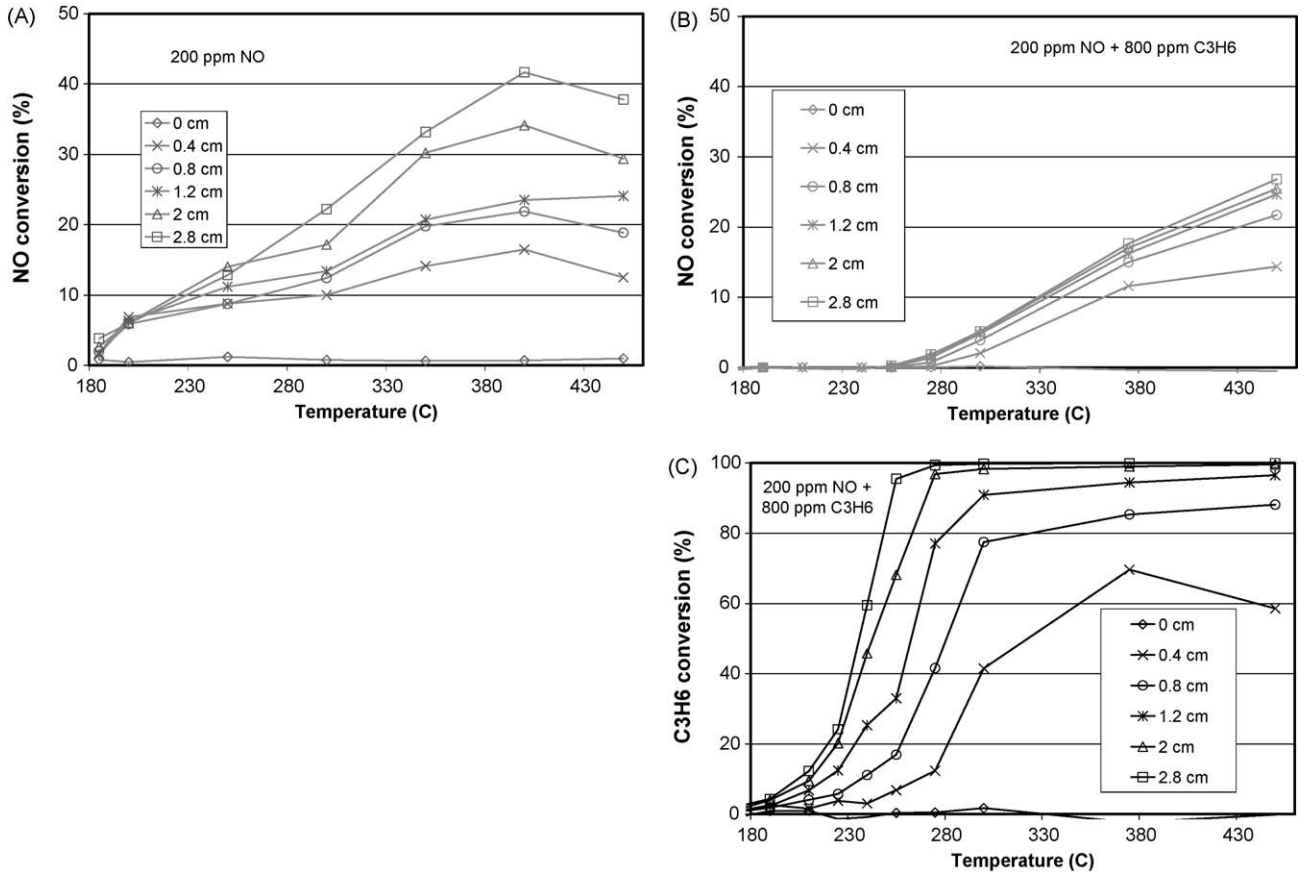

Fig. 2. NO and C_3H_6 oxidation conversion as a function of temperature and position (from the inlet) within the catalyst. The feed stream contained 200 ppm NO, 10% O_2, 5% H_2O and either (A) 0 ppm C_3H_6 or (B), (C) 800 ppm C_3H_6, and a balance of N_2.

concentration data presented in Fig. 1, the presence of C_3H_6 suppressed the maximum NO oxidation conversion. Furthermore, NO oxidation was primarily observed after C_3H_6 light-off, confirming severe NO oxidation inhibition in the presence of C_3H_6. From Fig. 2, we can also see that C_3H_6 oxidation began at the back of the catalyst and moved towards the front, with nearly 100% conversion observed at temperatures >255 °C within the front half of the catalyst. Furthermore, although at the intermediate higher temperatures C_3H_6 oxidation had lit off and primarily occurred in the front half of catalyst, the small amounts still being oxidized in the back half did suppress NO oxidation, in line with the data shown in Fig. 1, where small amounts still had a significant inhibiting effect.

There are several possibilities that could explain this inhibition effect. Simple competition for O_2 is unlikely since O_2 is present in large excess even at the highest C_3H_6 concentrations. Although, alkenes can lead to carbonaceous species that can poison Pt sites [39], it is not likely solely due to such poisoning since C_3H_6 oxidation begins at 150 °C (example data are shown in Fig. 1) and is almost completely converted above 260 °C, where the measured NO_2-out levels are still far smaller than those with no C_3H_6. Furthermore, it is not likely competition between C_3H_6 and NO for Pt sites, again because most of the C_3H_6 is consumed by 260 °C, yet NO oxidation is still suppressed at higher temperatures. The likely reason for the observed results is that the NO_2 formed is being consumed as an oxidant in the C_3H_6 oxidation reaction, resulting in the overall appearance of NO oxidation inhibition. Such a mechanism was proposed in an earlier study that demonstrated in the presence of CO and hydrocarbons, an aged commercial DOC will reduce NO_2 produced from NO oxidation, through its use as an oxidant for hydrocarbon and CO oxidation [36].

Experiments were run with NO_2 as the inlet NO_X source instead of NO in order to further study this phenomenon. Data obtained from a baseline NO_2 reduction experiment are shown in Fig. 3. The NO_2 concentration began decreasing at about 300 °C, which is a result of thermodynamic equilibrium between NO and NO_2 being attained over the catalyst. This is similar to the results obtained by Olsson et al. [18] where thermodynamic equilibrium between NO and NO_2 over Pt/Al_2O_3 catalysts was readily achieved at temperatures >350 °C. In Fig. 3 the effect of different hydrocarbons on NO_2 reduction, or what can also be considered as the use of NO_2 as the hydrocarbon oxidant is also shown. Because the three different hydrocarbons have different C-to-N ratios, the experiments were conducted with different concentrations resulting in each experiment having a comparable C:N ratio. 10% O_2 was also

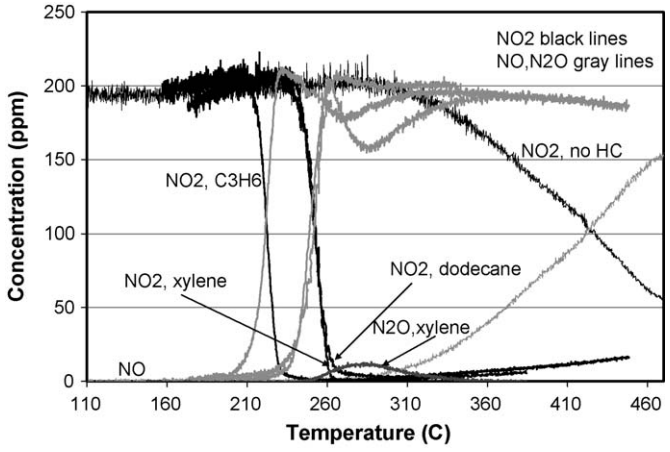

Fig. 3. NO_2 reduction as a function of temperature and hydrocarbon type. The feed stream contained 200 ppm NO_2, 10% O_2, 5% H_2O and either no HC or 800 ppm C_3H_6, 300 ppm C_8H_{10} or 200 ppm $C_{12}H_{26}$, and a balance of N_2.

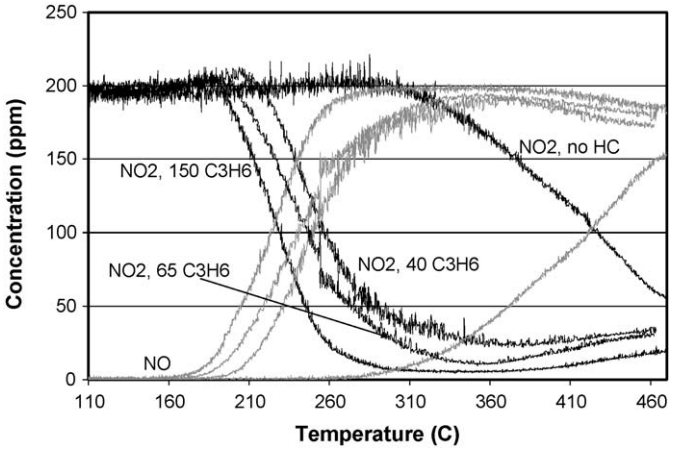

Fig. 4. NO_2 reduction as a function of temperature and C_3H_6 concentration. The feed stream contained 200 ppm NO_2, 10% O_2, 5% H_2O and either 0, 40, 65 or 150 ppm C_3H_6, and a balance of N_2.

present in each experiment. The addition of any of the three hydrocarbons used caused NO_2 reduction to occur at significantly lower temperatures than that seen in their absence. The primary product observed was NO, although some N_2O was observed after hydrocarbon oxidation and NO_2 reduction began, but dropped off as the hydrocarbons neared complete oxidation. An example of the N_2O formed during the m-xylene-containing experiment is plotted. Also, the formation of a small amount of N_2 via hydrocarbon SCR completes the mass balance on NO_X. For example, with m-xylene added, and at ~284 °C, the measured concentration of outlet NO and N_2O is ~159 and 11 ppm, respectively, while the inlet NO_2 was 202 ppm. Therefore, in order to close the mass balance, the concentration of N_2 must be approximately 10.5 ppm. Although equivalent C:N ratios were used, NO_2 reduction by C_3H_6 started at a lower temperature than that observed with $C_{12}H_{26}$ and m-xylene, whereas with these two larger molecules similar results were obtained. This demonstrates that the NO_2 reduction by the hydrocarbon, or NO_2 oxidation of the hydrocarbon, is dependent on the type of hydrocarbon itself. This will be further discussed below.

Different C_3H_6 levels were used to investigate the impact of hydrocarbon concentration on NO_2 reduction, with the data shown in Fig. 4. With every increase in propylene concentration, in the range examined, reduction began at a lower temperature. For example the temperature where C_3H_6 oxidation began shifted from 190 to 160 °C for 40 and 150 ppm, respectively. The extent of NO_2 reduction increased as well, with the minimum NO_2 dropping from 25 to 10 ppm. Furthermore, as more C_3H_6 was added, the temperature range across which reduction occurred became smaller. Both the smaller amount of NO_2 and the more rapid reduction as a function of temperature make sense as there is more reactant available for the reaction. These data show that the temperature where hydrocarbon oxidation via NO_2 begins is not only dependent on the hydrocarbon species (Fig. 3), but also on the amount of hydrocarbon present.

The experiment containing 200 ppm NO_2, 800 ppm C_3H_6, 10% O_2, 5% H_2O and N_2 as balance in the feed stream was also spatially resolved and the results are shown in Fig. 5. The onset of NO_2 reduction was observed between 175 and 200 °C, with low C_3H_6 conversions also noted in the same temperature range. In performing a mass balance at 200 °C, ~52% of the NO_2 was consumed. If NO_2 is only reduced to NO, and complete C_3H_6 combustion occurred via the NO_2 oxidant, then only ~12 ppm C_3H_6 would have been oxidized. However, the data indicate that ~20 ppm was oxidized. CO was observed in the outlet gas

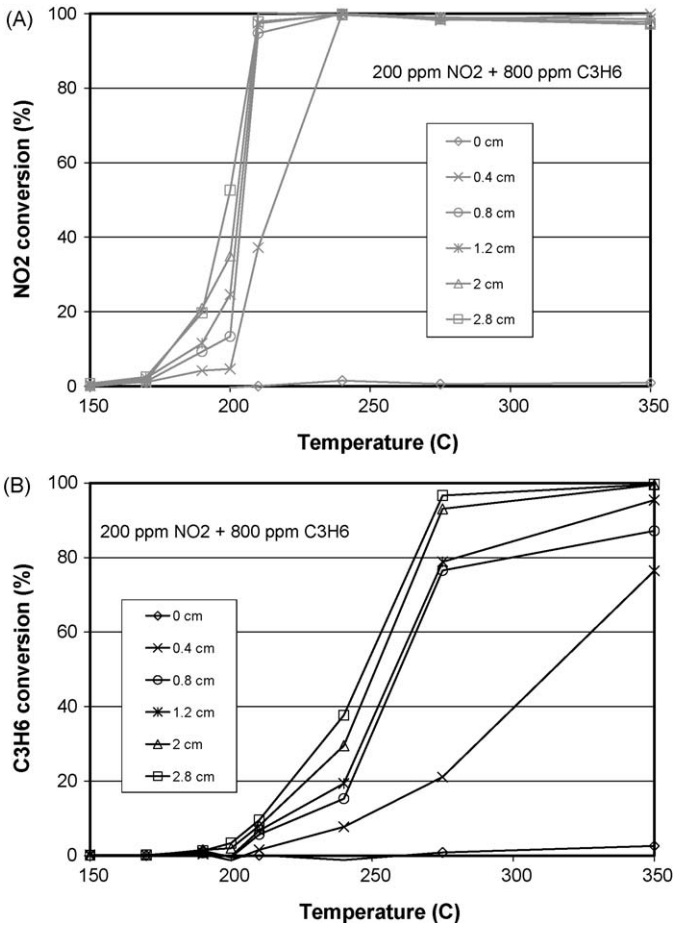

Fig. 5. (A) NO_2 reduction conversion, and (B) C_3H_6 oxidation conversion as a function of temperature and position (from the inlet) within the catalyst. The feed stream contained 200 ppm NO_2, 800 ppm C_3H_6, 10% O_2, 5% H_2O, and a balance of N_2.

composition in the hydrocarbon light-off temperature range accounting for at least some of the discrepancy. The CO concentrations within the catalyst, however, could not be resolved with the mass spectrometer. C_3H_6 oxidation by O_2 could also be occurring, which would of course make up the mass balance. At 210 °C, 100% NO_2 conversion was observed, with ~10% of the C_3H_6 consumed as well. Again, if NO was the product, a significantly smaller amount of C_3H_6 would have been oxidized, further indicating that O_2 is participating in the oxidation reaction by this temperature. At higher temperatures, it is clear that all the NO_2 was reduced within the very front portion of the catalyst.

The efficiency of NO_2 as the oxidant relative to O_2 was evaluated by studying the effect of different O_2 concentrations on NO_2 reduction and C_3H_6 oxidation. The NO_X data are plotted in Fig. 6. For this set of experiments the inlet C_3H_6 level was 150 ppm and the inlet NO_2 was 200 ppm. There was no significant change in the observed onset temperature for NO_2 reduction for the two cases with low O_2, suggesting that O_2 does not influence NO_2's participation in C_3H_6 oxidation. However, the test with higher O_2 concentration showed a lack of complete NO_2 reduction at the higher temperature, as well as a slightly slower drop in NO_2 as the temperature decreased, likely related to some NO oxidation beginning as well as the presence of large amounts of O_2 inhibiting the reduction via a shift in the equilibrium. Previous work has shown that with Pt/Al_2O_3 catalysts, a greater oxygen surface coverage exists in the presence of high O_2 concentrations, as well as in the presence of NO_2 since NO_2 is a strong oxidizer [18]. The onset at a slightly

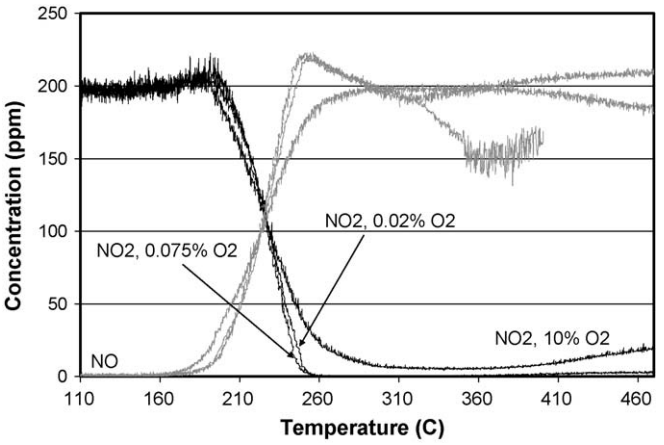

Fig. 6. NO_2 reduction as a function of temperature and O_2 concentration. The feed stream contained 200 ppm NO_2, 5% H_2O, 150 ppm C_3H_6, and either 0.02, 0.075 or 10% O_2 and a balance of N_2.

lower temperature is related to C_3H_6 oxidation beginning at a lower temperature as will be discussed below.

Almost all of the NO_2 is consumed in all the tests run, while with the high O_2 level runs, the O_2 is obviously not. This indicates that the NO_2 is being consumed preferentially relative to the O_2. For example, if NO_2 and O_2 were equal as oxidants, both would be consumed equally. The hydrocarbon balance, however, dictates that the O_2 is not being completely consumed. For 150 ppm C_3H_6 entering, only 675 ppm of O_2 would be required to consume all the C_3H_6. With 10% O_2 entering, this would mean less than 1% of the O_2 could be consumed, while still with 10% O_2 in the feed, more than 95% of the NO_2 is consumed, clearly demonstrating preferential use of the NO_2. This is further verified in the calculations presented above, associated with the data in Fig. 5, where complete NO_2 reduction occurred at the front portion of the catalyst while still within the C_3H_6 light-off temperature range.

The effect of varying the amount of O_2 on C_3H_6 oxidation is shown in Fig. 7. Two of the data sets plotted were run without NO_2 or NO in the feed stream. With the lower O_2 concentration (0.075% O_2), there is a 10% O_2 excess to facilitate complete C_3H_6 combustion. For the NO_X-free experiments, C_3H_6 light-off occurred at approximately the same temperature for the two O_2 levels tested. In the case with 10% oxygen, however, the decrease in C_3H_6 concentration was steeper and therefore occurred within a narrower temperature window, between about 185 and 250 °C, since there was significant excess O_2 in the feed. Also, complete

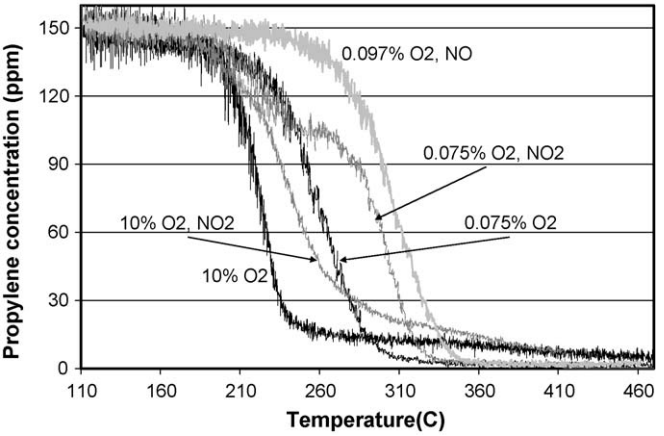

Fig. 7. C_3H_6 oxidation as a function of temperature, O_2 concentration and NO or NO_2 presence. The feed stream contained 5% H_2O, 150 ppm C_3H_6, with either 0.075 or 10% O_2, either 0 or 200 ppm NO_2 or 200 ppm NO and a balance of N_2.

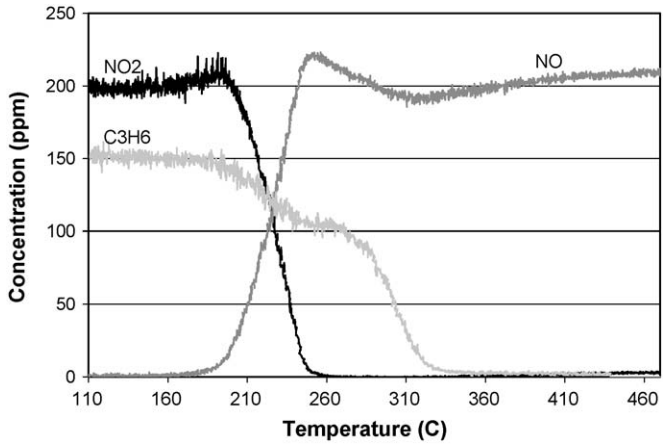

Fig. 8. C_3H_6 NO and NO_2 concentrations as a function of temperature. The feed stream contained 5% H_2O, 150 ppm C_3H_6, 0.075% O_2, 200 ppm NO_2 and a balance of N_2.

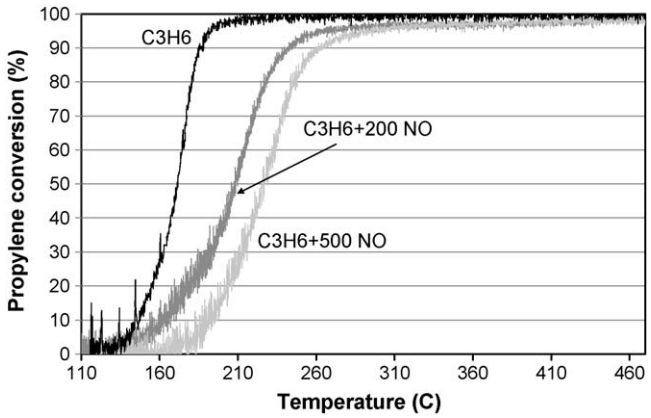

Fig. 9. C_3H_6 oxidation conversion as a function of temperature and NO concentration. The feed stream contained 5% H_2O, 200 ppm C_3H_6, 10% O_2, with either 0, 200 or 500 ppm NO and a balance of N_2.

combustion of C_3H_6 is observed with the lower O_2 experiment, but not with the higher. This could be due to the large amount of O_2 resulting in active site saturation, preventing the remaining C_3H_6 from reaching the surface, similar to the argument described above concerning the lack of complete NO_2 reduction. Such a phenomenon may be related to the sample's low precious metal loading, and therefore ease of site saturation.

In Fig. 7 the effect of adding NO_2 or NO on C_3H_6 oxidation is also shown. Propylene oxidation light-off occurred at the same temperature when NO_2 was or was not included with either 0.075% or 10% oxygen. The data shown in Fig. 6 indicated that O_2 had little to no effect on NO_2 reduction via C_3H_6 oxidation while the data in Fig. 3 indicated that the onset of NO_2 reduction depended on the hydrocarbon species. Also, the data in Fig. 4 showed that the onset of C_3H_6 oxidation varied with C_3H_6 level. Combined, these data demonstrate that the low temperature reaction constraint, or onset of the reaction, is activation of the C_3H_6 or hydrocarbon molecule.

In comparing the experiments with 0.075% O_2, the addition of NO_2 initially accelerates the C_3H_6 oxidation reaction, relative to no NO_2, but then inhibits it after light-off has occurred. This is especially evident in the 240–260 °C temperature range. This is not due to a switch between NO_2 and O_2 as oxidants, as the conversion is actually worse after 250 °C relative to the data obtained in the absence of NO_2. In the experiment with the 10% O_2 level, this apparent NO_2 inhibition effect is seen throughout the experiment (the temperature for 50% conversion is shifted upward by 22 °C). This negative effect is attributed to NO inhibition of the C_3H_6 oxidation reaction, with the NO formed from NO_2 reduction. As confirmation, the data obtained from an experiment with NO in the feed are also shown in Fig. 7. In this experiment, a slightly larger excess of O_2 was added to compensate for the O species lost with the removal of NO_2. The addition of NO caused C_3H_6 oxidation light-off to occur at a higher temperature, resulting in less C_3H_6 conversion across the entire temperature range, in comparison to any experiments not containing NO_X. For the experiments containing NO_2 and low-O_2, this is highlighted in Fig. 8. NO_2 reduction and C_3H_6 oxidation are clearly accompanied by the production of NO and the inflection in the C_3H_6 concentration profile is observed in the same temperature range where NO is produced. This inflection is more pronounced in the region where maximum NO is observed. Although N_2O was also produced in that same temperature range, it was only seen in the C_3H_6-containing experiments where lower O_2 concentrations were used and was not observed in the dataset obtained with 10% O_2 and therefore is not considered as the inhibiting factor. To further evaluate the inhibition of C_3H_6 oxidation by NO, experiments were conducted with varying NO concentrations, with the results presented in Fig. 9. Propylene light-off shifts to higher temperatures with increasing amounts of NO, confirming that NO inhibits C_3H_6 oxidation. Such an inhibition effect was also seen by Voltz et al. over Pt-containing catalysts [34]. Active site saturation by NO may be preventing C_3H_6 from reaching the surface, thus inhibiting C_3H_6 oxidation.

4. Conclusions

Hydrocarbons affect NO oxidation over a Pt-Pd/Al_2O_3 catalyst. Under the conditions of this study, increasing amounts of C_3H_6 resulted in lower NO conversion which was due to the consumption of product NO_2 as an oxidant in C_3H_6 oxidation. Such behaviour was confirmed by spatially resolving the species along the catalyst length as well as by studying the effect of increasing C_3H_6 concentrations and different hydrocarbon species on NO_2 reduction. The addition of hydrocarbons significantly decreased the NO_2 reduction temperature, as did increasing amounts of hydrocarbons. The onset of this reaction was correlated to the activation of the hydrocarbon species. Conversely, the presence of NO_2 initially accelerated C_3H_6 oxidation but inhibited it at higher temperatures due to the formation of NO, which was shown to inhibit C_3H_6 oxidation.

Acknowledgements

The authors would like to thank Natural Sciences and Engineering Research Council of Canada, General Motors and Ontario Centers of Excellence for their financial support. They would also like to acknowledge helpful discussions with Se Oh and Ed Bissett of the General Motors Research and Development Center.

References

[1] A. Neyestanaki, F. Klingstedt, T. Salmi, D. Murzin, Fuel 83 (2004) 395.
[2] M. Chen, L.D. Schmidt, Journal of Catalysis 56 (1979) 198.
[3] A. Morlang, U. Neuhausen, K.V. Klementiev, F.-W. Schu?tze, G. Miehe, H. Fuess, E.S. Lox, Applied Catalysis B: Environmental 60 (2005) 191.
[4] S. Erkfeldt, E. Jobson, M. Larsson, Topics in Catalysis 16/17 (2001) 127.
[5] F. Rodrigues, L. Juste, C. Potvin, J.F. Tempere, G. Blanchard, G. Djega-Mariadassou, Catalysis Letters 72 (2001) 59.
[6] N.W. Cant, M.J. Patterson, Catalysis Today 73 (2002) 271.
[7] S. Hodjati, P. Bernhardt, C. Petit, V. Pitchon, A. Kiennemann, Applied Catalysis B: Environmental 19 (1998) 209.
[8] S. Hodjati, K. Vaezzadeh, C. Petit, V. Pitchon, A. Kiennemann, Catalysis Today 59 (2000) 323.

[9] W.S. Epling, L.E. Campbell, A. Yezerets, N.W. Currier, J.E. Parks, Catalysis Reviews 46 (2004) 163.
[10] K.S. Kabin, R.L. Muncrief, M.P. Harold, Y. Li, Chemical Engineering Science 59 (2004) 5319.
[11] S. Salasc, M. Skoglundh, E. Fridell, Applied Catalysis B: Environmental 36 (2002) 145.
[12] H. Mahzoul, J.F. Brilhac, P. Gilot, Applied Catalysis B: Environmental 20 (1999) 47.
[13] F. Prinetto, G. Ghiotti, I. Nova, L. Lietti, E. Tronconi, P. Forzatti, Journal of Physical Chemistry B 105 (2001) 12732.
[14] S. Kikuyama, I. Matsukuma, R. Kikuchi, K. Sasaki, K. Eguchi, Applied Catalysis A: General 226 (2002) 23.
[15] P.J. Schmitz, R.J. Baird, Journal of Physical Chemistry B 106 (2002) 4172.
[16] Kato, S. Matsuda, T. Kamo, F. Nakajima, H. Kuroda, T. Narita, Journal of Physical Chemistry 85 (1981) 4099.
[17] J. Jung, S. Song and K. Min Chun, SAE Technical Paper Series 2008-01-0482.
[18] L. Olsson, B. Westerberg, H. Persson, E. Fridell, M. Skoglundh, B. Andersson, Journal of Physical Chemistry B 103 (1999) 10433.
[19] S.S. Mulla, N. Chen, W.N. Delgass, W.S. Epling, F.H. Ribeiro, Catalysis Letters 100 (2005) 267.
[20] S.S. Mulla, N. Chen, L. Cumaranatunge, G.E. Blau, D.Y. Zemlyanov, W.N. Delgass, W.S. Epling, F.H. Ribeiro, Journal of Catalysis 241 (2006) 389.
[21] J. Després, M. Elsener, M. Koebel, O. Kröcher, B. Schnyder, A. Wokaun, Applied Catalysis B: Environmental 50 (2004) 73.
[22] J. Segner, W. Vielhaber, G. Ertl, Israel Journal of Chemistry 22 (1982) 375.
[23] D.H. Parker, B. Koel, Journal of Vacuum Science and Technology A 8 (1990) 2585.
[24] J.-H. Lee, H.H. Kung, Catalysis Letters 51 (1998) 1.
[25] E. Xue, K. Seshan, J.R.H. Ross, Applied Catalysis B: Environmental 11 (1996) 65.
[26] P. Denton, A. Giroir-Fendler, H. Praliaud, M. Primet, Journal of Catalysis 189 (2000) 410.
[27] L. Olsson, E. Fridell, Journal of Catalysis 210 (2002) 340.
[28] S. Benard, L. Retailleau, F. Gaillard, P. Vernoux, A. Giroir-Fendler, Applied Catalysis B: Environmental 55 (2005) 11.
[29] L. Olsson, M. Abul-Milh, H. Karlsson, E. Jobson, P. Thormaehlen, A. Hinz, Topics in Catalysis 30/31 (2004) 85.
[30] M. Patterson, D. Angove, N. Cant, Applied Catalysis B: Environmental 26 (2000) 47.
[31] S. Ordóñez, L. Bello, H. Sastre, R. Rosal, F.V. Diez, Applied Catalysis B: Environmental 38 (2002) 139.
[32] A. Barresi, G. Baldi, Chemical Engineering Science 47 (1992) 1943.
[33] S. Salomons, R. Hayes, M. Votsmeier, Applied Catalysis A: General 52 (2009) 27.
[34] S. Voltz, C. Morgan, D. Liederman, S. Jacob, Industrial, Engineering Chemistry Product Research and Development 12 (1973) 294.
[35] S.R. Katare, J.E. Patterson, P.M. Laing, Industrial and Engineering Chemistry Research 46 (2007) 2445.
[36] S.R. Katare, J.E. Patterson, P.M. Laing, SAE Technical Paper Series 2007-01-3984.
[37] W. Partridge, J. Storey, S. Lewis, R. Smithwick, G. DeVault, M. Cunningham, N. Currier, T. Yonushonis, SAE Technical Paper Series 2000-01-2952.
[38] B. West, S. Huff, J. Parks, S. Lewis, J. Choi, W. Partridge, J. Storey, SAE Technical Paper Series 2004-01-3023.
[39] R. Burch, T.C. Watling, Catalysis Letters 43 (1997) 19.